Planar Triangular Resonators with Magnetic Walls

JOSEPH HELSZAJN, MEMBER, IEEE, AND DAVID S. JAMES, MEMBER, IEEE

Abstract—**This paper gives the field patterns in triangular planar resonators having no variation of the fields along the substrate thickness. The TM fields in such resonators with magnetic boundary conditions are obtained by duality from the TE modes with electric boundaries. The theoretical description includes the cutoff numbers of the first few modes. The radiation Q factor of fundamental microstrip resonators of this type was found experimentally to be higher than that associated with conventional disk resonators. The performance of a microstrip circulator using a triangular resonator is also described.**

I. Introduction

THIS PAPER DESCRIBES theoretical and experimental results on planar resonators of equilateral triangle shape and having magnetic sidewalls (Fig. 1).

The TM field patterns and cutoff numbers of such ferrite or dielectric resonators with magnetic boundary conditions are obtained by duality from those of TE modes with electric boundary conditions [1]–[3]. These field patterns have not previously been described in the literature. A table of the properties of the dominant and some higher order modes is also included.

Good agreement is observed between the measured and theoretical electric field distribution at the edge of a loosely coupled microstrip resonator operating in the dominant mode.

The radiation loss of this type of resonator has been studied experimentally and compared with that obtained using disk resonators. Preliminary results for the dominant mode indicate that this resonator has somewhat less radiation loss than the disk resonator. The resultant higher unloaded Q factor for this geometry makes it particularly attractive for use in circulator designs.

To establish the suitability of triangular resonators for component use, experimental microstrip circulators have been constructed which incorporate such resonators instead of the conventional disk ones. The experimental results indicate that circulators built with triangular resonators have lower radiation losses and increased bandwidths compared with those of conventional circulators.

Manuscript received July 19, 1976; revised June 24, 1977.

J. Helszajn is with the Department of Electrical and Electronic Engineering, Heriot-Watt University, Edinburgh, EH1 2HT, Scotland.

D. S. James was with the Communications Research Centre, Department of Communications, Ottawa, K2H 8S2. He is now with Ferranti Solid-State Microwave, Manchester, M22 4RN, England.

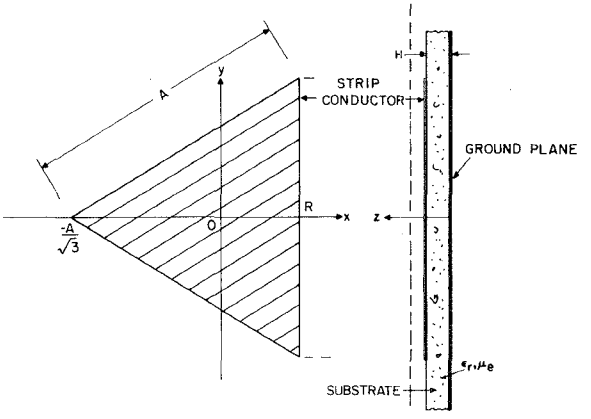

Fig. 1. Schematic of microstrip triangular resonator. Dotted line shows extra ground plane for stripline.

II. TM Field Patterns of Triangular Planar Resonator

The TM-mode field patterns in a triangular-shaped demagnetized ferrite or dielectric resonator having no variation of the field patterns along the thickness of the resonator are given by

$$E_z = A_{m,n,1}\, T(x,y) \tag{1}$$

$$H_x = \frac{j}{\omega \mu_0 \mu_e} \frac{\delta E_z}{\delta y} \tag{2}$$

$$H_y = \frac{-j}{\omega \mu_0 \mu_e} \frac{\delta E_z}{\delta x} \tag{3}$$

$$H_z = E_x = E_y = 0 \tag{4}$$

where $A_{m,n,1}$ is a constant. Fig. 1 shows the geometry of the planar resonator discussed in this text.

For magnetic boundary conditions, $T(x,y)$ may be obtained by duality from that of the TE mode with electric boundary conditions [1]–[3]:

$$T(x,y) = \cos\left[\left(\frac{2\pi x}{\sqrt{3A}} + \frac{2\pi}{3}\right)1\right]\cos\left[\frac{2\pi(m-n)y}{3A}\right] + \cos\left[\left(\frac{2\pi x}{\sqrt{3A}} + \frac{2\pi}{3}\right)m\right]\cos\left[\frac{2\pi(n-1)y}{3A}\right] + \cos\left[\left(\frac{2\pi x}{\sqrt{3A}} + \frac{2\pi}{3}\right)n\right]\cos\left[\frac{2\pi(1-m)y}{3A}\right] \tag{5}$$

where A is the length of the triangle side and

$$m + n + 1 = 0 \tag{6}$$

which satisfies the wave equation

$$\left(\frac{\delta^2}{\delta x^2} + \frac{\delta^2}{\delta y^2} + k_{m,n,1}^2\right) E_z = 0 \tag{7}$$

where

$$k_{m,n,1} = \frac{4\pi}{3A} \cdot \sqrt{m^2 + mn + n^2}. \tag{8}$$

The complete standing wave solution is

$$E_z = A_{m,n,1}\, T(x,y) \tag{9}$$

$$\begin{aligned} H_x = \frac{-jA_{m,n,1}}{\omega\mu_0\mu_e} \Bigg\{ & \frac{2\pi(m-n)}{3A} \cos\left[\left(\frac{2\pi x}{\sqrt{3}A} + \frac{2\pi}{3}\right)1\right] \\ & \cdot \sin\left[\frac{2\pi(m-n)y}{3A}\right] + \frac{2\pi(n-1)}{3A} \\ & \cdot \cos\left[\left(\frac{2\pi x}{\sqrt{3}A} + \frac{2\pi}{3}\right)m\right] \\ & \cdot \sin\left[\frac{2\pi(n-1)y}{3A}\right] + \frac{2\pi(1-m)}{3A} \\ & \cdot \cos\left[\left(\frac{2\pi x}{\sqrt{3}A} + \frac{2\pi}{3}\right)n\right] \sin\left[\frac{2\pi(1-m)y}{3A}\right] \Bigg\} \end{aligned} \tag{10}$$

$$\begin{aligned} H_y = \frac{jA_{m,n,1}}{\omega\mu_0\mu_e} \Bigg\{ & \frac{2\pi 1}{\sqrt{3}A} \sin\left[\left(\frac{2\pi x}{\sqrt{3}A} + \frac{2\pi}{3}\right)1\right] \\ & \cdot \cos\left[\frac{2\pi(m-n)y}{3A}\right] + \frac{2\pi m}{\sqrt{3}A} \sin\left[\left(\frac{2\pi x}{\sqrt{3}A} + \frac{2\pi}{3}\right)m\right] \\ & \cdot \cos\left[\frac{2\pi(n-1)y}{3A}\right] + \frac{2\pi n}{\sqrt{3}A} \\ & \cdot \sin\left[\left(\frac{2\pi x}{\sqrt{3}A} + \frac{2\pi}{3}\right)n\right] \cos\left[\frac{2\pi(1-m)y}{3A}\right] \Bigg\}. \end{aligned} \tag{11}$$

It is observed that the interchange of the three digits $m,n,1$ leaves the cutoff number $k_{m,n,1}$ unchanged; similarly, the field patterns are retained, without rotation.

III. $TM_{1,0,-1}$ Field Components of Triangular Planar Resonator

The dominant mode in a planar triangular resonator is given by (9)–(11) with $m = 1$, $n = 0$, $1 = -1$. The result is

$$\begin{aligned} E_z = A_{1,0,-1} \Bigg[& 2\cos\left(\frac{2\pi x}{\sqrt{3}A} + \frac{2\pi}{3}\right) \\ & \cdot \cos\left(\frac{2\pi y}{3A}\right) + \cos\left(\frac{4\pi y}{3A}\right) \Bigg] \end{aligned} \tag{12}$$

$$\begin{aligned} H_x = -jA_{1,0,-1}\zeta_e \Bigg[& \cos\left(\frac{2\pi x}{\sqrt{3}A} + \frac{2\pi}{3}\right) \\ & \cdot \sin\left(\frac{2\pi y}{3A}\right) + \sin\left(\frac{4\pi y}{3A}\right) \Bigg] \end{aligned} \tag{13}$$

$$H_y = j\sqrt{3}\, A_{1,0,-1}\zeta_e \left[\sin\left(\frac{2\pi x}{\sqrt{3}A} + \frac{2\pi}{3}\right) \cos\left(\frac{2\pi y}{3A}\right)\right] \tag{14}$$

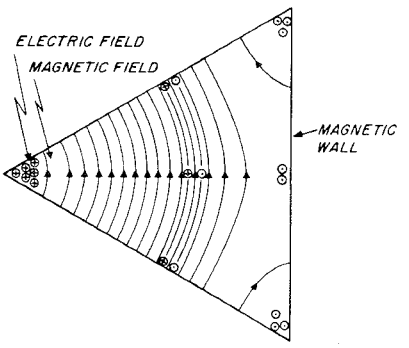

Fig. 2. $TM_{1,0,-1}$ dominant mode field pattern in triangular resonator with magnetic walls.

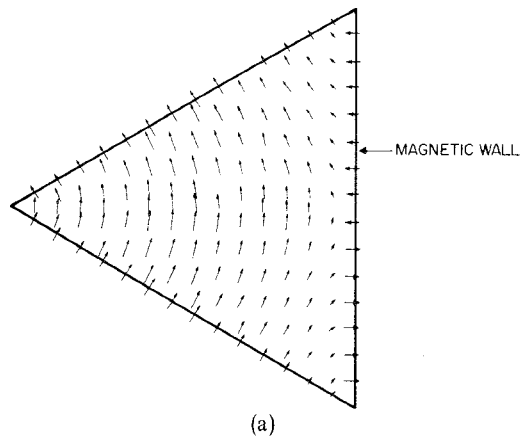

Fig. 3. (a) Magnetic field pattern for dominant mode. (b) Lines of equipotential. $A_{1,0,-1} = 1$ assumed.

where

$$k = \frac{4\pi}{3A} \tag{15}$$

$$\zeta_e = \sqrt{\frac{\varepsilon_0\varepsilon_r}{\mu_0\mu_e}}. \tag{16}$$

Fig. 2 is a sketch of the magnetic and electric fields for the dominant $TM_{1,0,-1}$ mode in a triangular resonator, and Fig. 3(a) and 3(b) indicate the corresponding magnetic field and equipotential lines. There are some differences between the pattern in Figs. 2 and 3 and that in Fig. 14 presented by

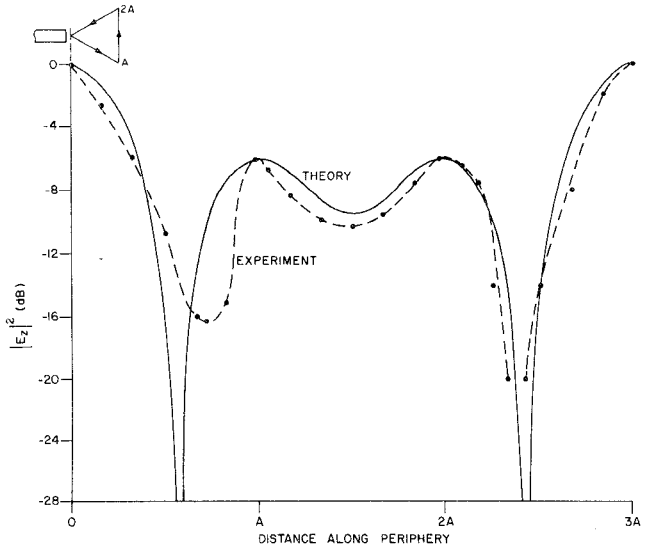

Fig. 4. Theoretical and experimental electric field distribution at edge of loosely coupled $TM_{1,0,-1}$ triangular resonator on alumina substrate, 9.2 GHz.

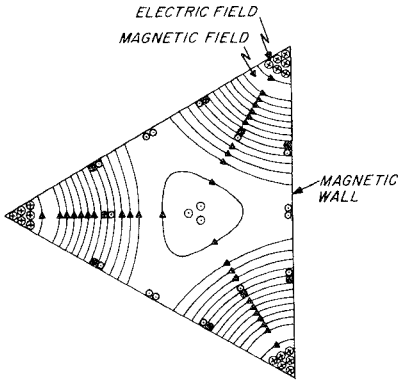

Fig. 5. $TM_{1,1,-2}$ field pattern in triangular resonator with magnetic walls.

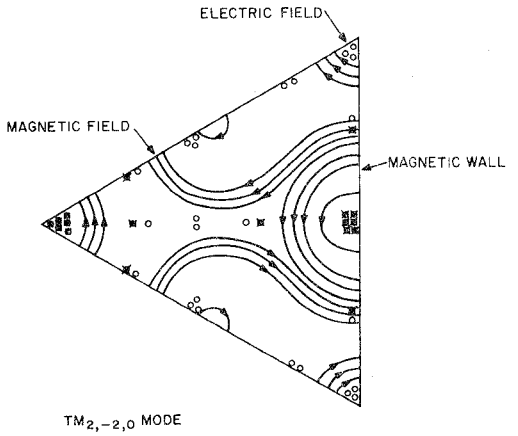

Fig. 6. $TM_{2,-2,0}$ field pattern in triangular resonator with magnetic walls.

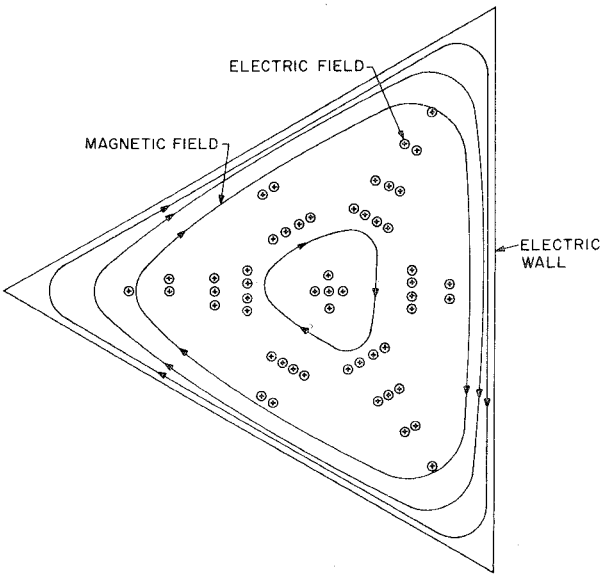

Fig. 7. $TE_{1,1,-2}$ field pattern in triangular resonator with electric walls.

Akaiwa [2]. Fig. 4 gives the measured and predicted electric field distribution at the periphery of a loosely coupled resonator operating in the $TM_{1,0,-1}$ mode.

IV. $TM_{1,1,-2}$ Field Components of Triangular Planar Resonator

In addition to the dominant mode the next higher order mode in a planar triangular resonator has also been investigated. This next mode is a symmetrical or in-phase one for which the field patterns are given in Fig. 5.

This in-phase mode is obtained with $m = 1$, $n = 1$, $1 = -2$; $T(x,y)_{m,n,1}$, and $k_{m,n,1}$ are therefore

$$T(x,y)_{1,1,-2} = \cos 2\left(\frac{2\pi x}{\sqrt{3}A} + 2\pi/3\right) + 2\cos\left(\frac{2\pi x}{\sqrt{3}A} + 2\pi/3\right)\cdot\cos\left(\frac{2\pi y}{A}\right) \quad (17)$$

$$k_{1,1,-2} = \frac{4\pi}{\sqrt{3}A}. \quad (18)$$

This mode has the property that $|T(x,y)_{1,1,-2}|$ has a maximum at the origin, unlike $T(x,y)_{1,0,-1}$ which has a zero there. This maximum is given by

$$T(0,0)_{1,1,-2} = \frac{-3}{2}. \quad (19)$$

It is easily verified that this mode is symmetrical, e.g.,

$$T(0,A/2\sqrt{3})_{1,1,-2} = T(-A/4\sqrt{3},A/4)_{1,1,-2} = T(-A/4\sqrt{3},-A/4)_{1,1,-2}. \quad (20)$$

The next higher order mode, which is the $TM_{2,-2,0}$ mode, has also been evaluated, and is illustrated in Fig. 6.

For comparison, Fig. 7 gives the field pattern of the symmetrical $TE_{1,1,-2}$ mode in a triangular resonator which has electric instead of magnetic sidewalls.

V. Boundary Condition of Planar Triangular Resonator

The resonant frequency of the open triangular demagnetized ferrite or dielectric resonator may be obtained from

TABLE I
$TM_{m,n,1}$ MODES FOR TRIANGULAR RESONATORS

Sequence no.	m, n, l	$k_{m,n,l} \cdot 3A/4\pi$	$\int_S [T(x,y)_{m,n,l}]^2 dS$
1 (dominant)	1, 0, -1	1	$9\sqrt{3}/2$
2 (symmetric)	1, 1, -2	$\sqrt{3}$	"
3	2, -2, 0	2	"
4	1, 2, -3	$\sqrt{7}$	$9\sqrt{3}/4$
5	3, -3, 0	3	$9\sqrt{3}/2$
6	2, 2, -4	$2\sqrt{3}$	"
7	1, 3, -4	$\sqrt{13}$	$9\sqrt{3}/4$
8	2, 3, -5	$\sqrt{19}$	"
9	1, 4, -5	$\sqrt{21}$	"

(8) or by establishing a magnetic wall at the edge of the resonator using the standing wave form of the field patterns.

Since the boundary condition must be satisfied at any point on the edge of the resonator, the convenient coordinates $x = -A/3$ and $y = 0$ are chosen in the first instance and it is verified that the cutoff number obtained there applies everywhere else also.

Setting $H_y = 0$, using the above coordinates gives for $m = 1, 1 - 0$, and $n = -1$

$$k_{1,0,-1} = \frac{4\pi}{3A} \tag{21}$$

or

$$\frac{2\pi\sqrt{\varepsilon_r \mu_e}}{\lambda_0} = \frac{4\pi}{3A} \tag{22}$$

where A is the side of the triangle (Fig. 1). Likewise, $H_y = 0$ at $x = R$ for all values of y with the value of k defined above.

A magnetic wall is also established on the slanted sides of the triangle such that

$$H_y \sin 30^\circ + H_x \cos 30^\circ = 0. \tag{23}$$

From measurements of the resonant frequencies for the first few modes of loosely coupled microstrip resonators, the effective value of the triangle side A_{eff} is observed to be given to good approximation by the following semiempirical expression:

$$A_{\text{eff}} = A + pH. \tag{24}$$

The second term in the above expression accounts for the fringing fields associated with the fact that the boundary condition at the edges of the microstrip resonator is not in practice an ideal magnetic wall; with alumina ($\varepsilon_r = 10$)$p \approx 1/3$, and with garnet ($\varepsilon_r = 15$)$p \approx 1/4$ for $A/H \geq 4$.

Table I gives the cutoff numbers for the first few modes together with the corresponding values for the integral $\int_S [T(x,y)_{m,n,1}]^2\, dS$. The latter is related to the resonator's stored energy as

$$W_{m,n,1} = \frac{A^2_{m,n,1}\, \varepsilon_0 \varepsilon_r A^2 H}{24} \int_S [T(x,y)_{m,n,1}]^2\, dS. \tag{25}$$

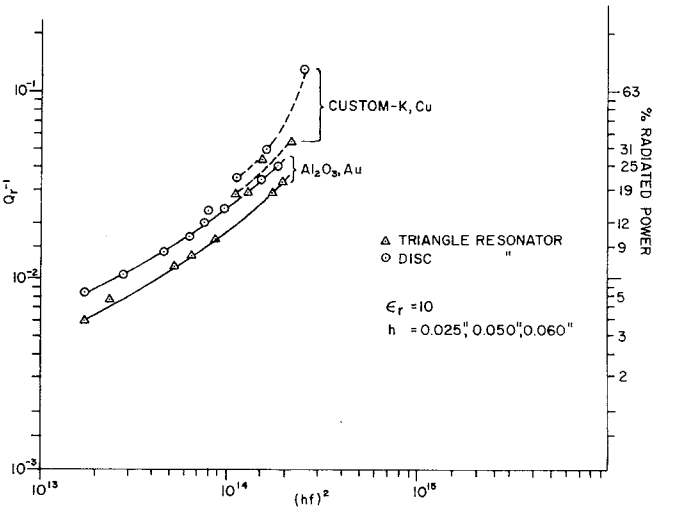

Fig. 8. Measured radiation Q's for dominant TM modes of triangular and disk-shaped microstrip resonators.

In turn, knowledge of this stored energy value would be used in the calculation of the appropriate coupling factor for various coupling structures for the resonator [4], and similarly in the calculation of the normalized power radiated from the resonator [5]–[10].

VI. Unloaded Q Factor of Open Triangular Dielectric Resonators

The total unloaded Q factor of an open dielectric resonator is made up of contributions due to dielectric losses Q_d, magnetic losses Q_m, conductor losses Q_c, and radiation losses Q_r. It is given by [10]

$$\frac{1}{Q_u} = \frac{1}{Q_c} + \frac{1}{Q_d} + \frac{1}{Q_m} + \frac{1}{Q_r}. \tag{26}$$

Provided there is no variation of the fields along the thickness of the resonator, the conductor loss is independent of the mode pattern and is given by [7].

$$Q_c = \sqrt{2\omega\mu_0\sigma}\, H \tag{27}$$

where σ is the conductivity and the other variables have the usual meaning. Likewise, the dielectric and magnetic losses are given in the standard way by

$$Q_d = \frac{1}{\varepsilon_r''} \tag{28}$$

$$Q_m = \frac{1}{\mu_r''} \tag{29}$$

where ε_r'' and μ_e'' are the imaginary parts of the permittivity and permeability, respectively.

Although no analytical expression is available for the Q factor associated with the radiation loss of the triangular open dielectric resonator, it may be obtained experimentally by measuring the overall unloaded Q factor of the resonator with and without a low-loss shielding enclosure [5]. Fig. 8 presents some experimental results for triangular and disk-shaped microstrip resonators operated in the dominant $TM_{1,0,-1}$ and $n = 1$ [7] modes, respectively. Both these

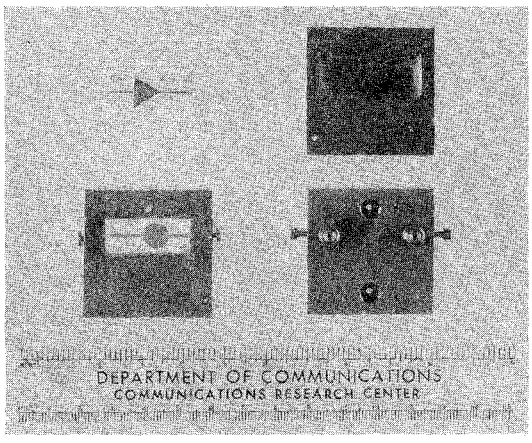

Fig. 9. Configurations used for Q_r tests on microstrip disk and triangular resonators.

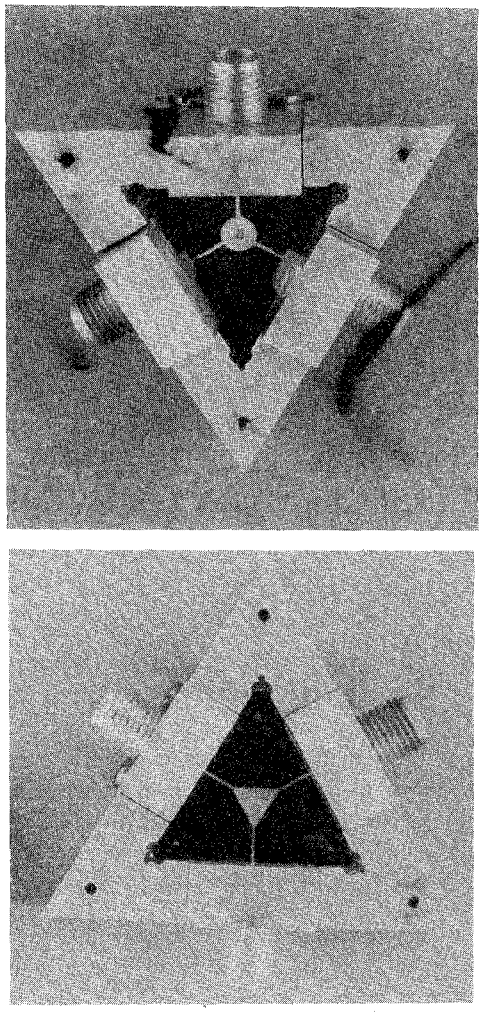

Fig. 10. Microstrip circulators using circular and triangular resonators.

modes have nonsymmetric field patterns. Most of the Q_r measurements were undertaken on Ti : W–Au coated substrates, although some tests utilized copper-clad boards. The substrates varied in thickness from 0.6 to 1.5 mm, with the resonators excited as shown in Fig. 9. The orthogonal type of launcher mounting shown consistently provides lower undesired radiation and surface wave propagation than that for the conventional in-line launcher. The input and output coupling factors for each resonator were empirically equalized to give typical insertion losses of around 15 dB. No difficulties were experienced with mode degeneracy.

The results suggest that the radiation Q for triangular resonators exceed that associated with the conventional disk resonators, although the difference is certainly not dramatic. Both geometries provide Q_r values inferior to that for linear, U-shaped, or ring types [9], but each provides the symmetry and mode patterns necessary for 3-port junction devices. Furthermore, it has been experimentally verified that the Q_r value for a microstrip triangular resonator on garnet also applies to the split $TM_{1,0,-1}$ modes generated by application of a bias field.

VII. Circulator and Filter Circuits Using Triangular Resonators

Stripline or microstrip circulators may be designed to utilize triangular rather than disk-shaped junctions. For the triangle junction the two counter-rotating modes used are the split $TM_{1,0,-1}$ modes, and the symmetric or in-phase third mode is the $TM_{1,1,-2}$ mode.

Fig. 10 illustrates practical X-band microstrip circulators using triangular and disk resonators. The substrate used was a garnet with a saturation magnetization of 0.1200 Wb/m^2 and a dielectric constant of 15.2. The substrate thickness was 0.635 mm, while the width of the top conductor for the 50 microstrip lines was 0.30 mm. The A dimension of the triangle resonator was 6.60 mm. Fig. 11 indicates the measured isolation and insertion loss for this junction. The insertion loss is 0.50-dB maximum and the bandwidth at the 20-dB points is 8.8 percent. This compares with an

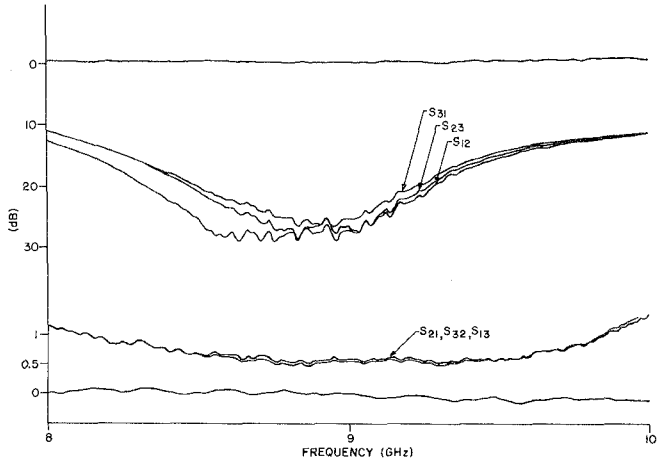

Fig. 11. Measured isolation and insertion loss.

insertion loss of 0.60 dB and a bandwidth of 4.4 percent for a conventional disk circulator built on a similar substrate. For the circulator using the triangular resonator the ferrite loss is 0.28 dB and the circuit loss is 0.22 dB, while for the circular geometry, the ferrite loss is 0.27 dB and the circuit dissipation is 0.32 dB [11]. With the triangular geometry, the

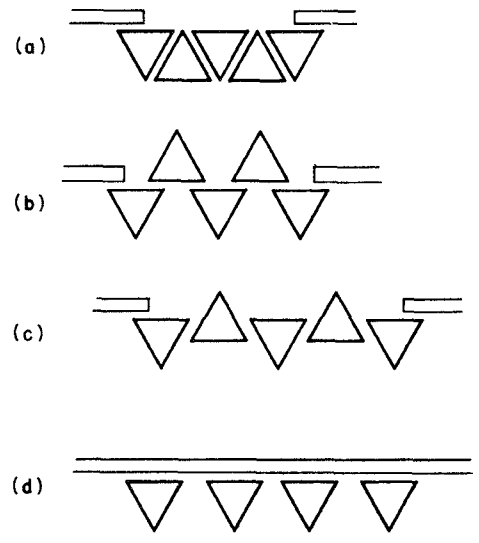

Fig. 12. (a), (b), (c) Band-pass filter schematics. (d) Band-stop filter schematics.

circulator center frequency is lower than that predicted by (22) and (24), due to the effect of the coupling lines at the resonator vertices.

Triangular resonators appear to hold some promise as prototype elements for filter circuits. Fig. 12(a)–(c) depicts three possible band-pass arrangements, while Fig. 12(d) illustrates a bandstop network. The coupling between such resonators has not been determined at this time.

VIII. Conclusions

This paper has presented a theoretical and experimental description of planar triangular resonators. It includes the investigation of some lower order field patterns and cutoff numbers for these resonators. For the fundamental mode in microstrip, the radiation loss for this type of geometry has been studied experimentally and found to be somewhat lower than that obtained with circular resonators. An experimental circulator using a triangular junction is also described.

Acknowledgment

The authors would like to thank M. Cuhaci for the Q_r measurements, and R. Marchand, E. Minkus, F. Bouchard, and members of the Microelectronics Group at the Communications Research Centre for considerable assistance.

References

[1] S. A. Schelkunoff, *Electromagnetic Waves*. New York: Van Nostrand, 1943, p. 393.
[2] Y. Akaiwa, "Operation modes of a waveguide Y-circulator," *IEEE Trans. Microwave Theory Tech.*, vol. MTT-22, pp. 954–959, Nov. 1974.
[3] N. Ogasawara and T. Noguchi, "Modal analysis of dielectric resonator of the normal triangular cross-section," presented at the 1974 Annual National Convention of the IEEE, Japan, Mar. 28, 1974.
[4] H. A. Wheeler, "Coupling holes between resonant cavities or waveguides evaluated in terms of volume ratios," *IEEE Trans. Microwave Theory Tech.*, vol. MTT-12, pp. 231–244, Mar. 1964.
[5] B. Easter and R. J. Roberts, "Radiation from half wavelength open circuit microstrip resonators," *Electronics Letters*, vol. 6, no. 18, pp. 573–574, Sept. 3, 1970.
[6] E. Belohoubek and E. Denlinger, "Loss considerations for microstrip resonators," *IEEE Trans. Microwave Theory Tech.*, vol. MTT-23, pp. 522–526, June 1975.
[7] J. Watkins, "Circular resonant structures in microstrip," *Electronics Letters*, vol. 5, no. 21, pp. 524–525, 1969.
[8] E. J. Denlinger, "Radiation from microstrip resonators," *IEEE Trans. Microwave Theory Tech.*, vol. MTT-17, pp. 235–236, Apr. 1969.
[9] R. J. Roberts and B. Easter, "Microstrip resonators having reduced radiation loss," *Electronics Letters*, vol. 7, no. 8, pp. 191–192, Apr. 22, 1971.
[10] J. Watkins, "Radiation loss from open-circuited dielectric resonators," *IEEE Trans. Microwave Theory Tech.*, vol. MTT-21, pp. 636–639, Oct. 1973.
[11] J. Helszajn, G. P. Riblet, and J. R. Mather, "Insertion loss of 3-port circulator with one port terminated in variable short circuit," *IEEE Trans. Microwave Theory Tech.*, vol. MTT-23, Nov. 1975.